HHS Public Access

Author manuscript

Brain Res. Author manuscript; available in PMC 2016 October 05.

Published in final edited form as:

Brain Res. 2015 October 5; 1622: 51–63. doi:10.1016/j.brainres.2015.06.011.

A pivotal role for enhanced brainstem Orexin receptor 1 signaling in the central cannabinoid receptor 1-mediated pressor response in conscious rats

Badr Mostafa Ibrahim and **Abdel A. Abdel-Rahman***

Department of Pharmacology & Toxicology, Brody School of Medicine, East Carolina University, 600 Moye Boulevard, Greenville, NC 27858, United States

Abstract

Orexin receptor 1 (OX_1R) signaling is implicated in cannabinoid receptor 1 (CB_1R) modulation of feeding. Further, our studies established the dependence of the central CB_1R-mediated pressor response on neuronal nitric oxide synthase (nNOS) and extracellular signal-regulated kinase1/2 (ERK1/2) phosphorylation in the RVLM. We tested the novel hypothesis that brainstem orexin-A/OX_1R signaling plays a pivotal role in the central CB_1R-mediated pressor response. Our multiple labeling immunofluorescence findings revealed co-localization of CB_1R, OX_1R and the peptide orexin-A within the C1 area of the rostral ventrolateral medulla (RVLM). Activation of central CB_1R following intracisternal (i.c.) WIN55,212-2 (15 μg/rat) in conscious rats caused significant increases in BP and orexin-A level in RVLM neuronal tissue. Additional studies established a causal role for orexin-A in the central CB_1R-mediated pressor response because (i) selective blockade of central CB_1R (AM251, 30 μg/rat; i.c.) abrogated WIN55,212-2-evoked increases in RVLM orexin-A level, (ii) the selective OX_1R antagonist SB-408124 (10 nmol/rat; i.c.) attenuated orexin-A (3 nmol/rat; i.c.) or WIN55,212-2 (15 μg/rat; i.c.)-evoked pressor response while selective CB_1R blockade (AM251) had no effect on orexin-A (3 nmol/rat; i.c.)-evoked pressor response, (iii) direct CB_1R activation in the RVLM (WIN55,212-2; 0.1 μg/rat) increased RVLM orexin-A and BP. Finally, SB-408124 attenuated WIN55,212-2-evoked increases in RVLM nNOS and ERK1/2 phosphorylation and BP. Our findings suggest that orexin-A/OX_1R dependent activation of the RVLM nNOS/ERK1/2 cascade is essential neurochemical mechanism for the central CB_1R–mediated pressor response in conscious rats.

Keywords

Blood pressure; Cannabinoid receptor 1; Orexin receptor 1; Rostral ventrolateral medulla

1. Introduction

Our recent studies implicated the activation (phosphorylation) of the neuronal nitric oxide synthase (nNOS) and extracellular signal-regulated kinase1/2 (ERK1/2) in the central

*Corresponding author. Fax: +1 252 744 3203., abdelrahmana@ecu.edu (A.A. Abdel-Rahman).

Conflict of interest

The authors declare no conflict of interest.

cannabinoid receptor 1 (CB_1R)-evoked pressor response in conscious freely moving rats (Ibrahim and Abdel-Rahman, 2012a, 2012b). However, the exact mechanisms of such response remain unclear. In the CNS, CB_1R activation suppresses synaptic transmission of inhibitory GABAergic, and enhances excitatory glutamatergic (Drew et al., 2008; Freund et al., 2003; Piomelli, 2003) and orexinergic (Huang et al., 2007; Matias et al., 2008; Verty et al., 2009) neurotransmission in various brain areas. This premise raises the interesting possibility that alterations in excitatory/inhibitory inputs in the rostral ventrolateral medulla (RVLM), the brainstem pressor region from which bulbospinal sympathetic neurons descend to the intermediolateral cell column of the spinal cord (Chalmers and Pilowsky, 1991; Padley et al., 2003; Pilowsky and Goodchild, 2002), underlie the central CB_1R-evoked pressor response.

Notably, an interaction between CB_1R and Orexin receptor 1 (OX_1R) (Ellis et al., 2006; Hilairet et al., 2003; Ward et al., 2011a, 2011b) contributes to feeding regulation. The CB_1R-OX_1R interaction is neurobiologically relevant because feeding evoked by orexin-A, an endogenous agonist of orexin receptors (also known as hypocretin-1), was abrogated by CB_1R blockade (Crespo et al., 2008). It is not known if a similar functionally relevant CB_1R-OX_1R interaction occurs in cardiovascular controlling areas in the brainstem. Although orexin-A expressing neurons are exclusive to the hypothalamus, orexin-A immunoreactive fibers (orexin-A-ir) exist in close proximity to catecholamine (C1) neurons in the RVLM (Ciriello et al., 2003a; Machado et al., 2002; Puskás et al., 2010; Shahid et al., 2012). Importantly, the expression of CB_1R exhibits similar patterns in the RVLM (Herkenham et al., 1991; Padley et al., 2003); however, there are no attempts made to directly investigate the potential colocalization of the two receptors in the RVLM. While most of the in vivo studies on OX_1R signaling dealt with feeding behavior and energy homeostasis, few studies showed that orexin-A elicits pressor response following its intracisternal (Chen et al., 2000; Zhang et al., 2005), intracerebroventricular (Samson et al., 1999; Shirasaka et al., 1999) or intra-RVLM (Chen et al., 2000; Ciriello et al., 2003a; Machado et al., 2002; Shahid et al., 2012) injections.

The aim of the present study was to test the hypothesis that enhanced brainstem orexin-A/OX_1R signaling is an essential molecular event for the central CB_1R-mediated pressor response. First, we determined if the CB_1R is colocalized with OX_1R and/or the peptide orexin-A in catecholamine expressing (C1) neurons of the RVLM. Second, we conducted integrative cardiovascular studies with selective CB_1R and OX_1R agonists and antagonists microinjected intracisternally or directly into the RVLM. Third, we conducted ex vivo measurements of orexin-A and nNOS and ERK1/2 phosphorylation levels in the RVLM following the pharmacological interventions used in the integrative studies. The pharmacological and neurochemical findings established a causal role for RVLM orexin-A/OX_1R signaling in the central CB_1R-mediated pressor response.

2. Results

2.1. Colocalization of orexin-A/OX_1R and CB_1R in rat RVLM

Coronal brainstem sections from naïve non-treated animals (n=4) were prepared for multiple co-localization of CB_1R/ orexin-A or TH/OX_1R/CB_1R within the C1 area of RVLM, as

described under methods and in our previous studies (Ibrahim and Abdel-Rahman, 2011, 2012b). Dual labeling immunofluorescence studies in the RVLM (Fig. 1A and B) revealed CB_1R-ir presynaptic punctate-structures (green) in close proximity to, or colocalized with, orexin-A-ir fibers (red) (Fig. 1C; arrows). Yet, in rare cases, we observed a CB_1R-ir somatodendritic apposition to orexin-A fibers marked by asterisk in Fig. 1C. The majority of TH-ir neurons exhibited CB_1 and OX_1 receptors immunoreactivity although CB_1R immunoreactivity was also evident outside of TH-ir neurons (Fig. 2A–D), which is consistent with the axonal and astrocytic labeling seen in other CNS sites. Fig. 2E shows the average of counted immunoreactive neurons/section (15–24 sections/ animal; *n*=4) within the VLM area −11.8 mm rostral to −12.6 mm caudal from the bregma. Notably, the majority of TH-ir neurons (1187/1389 neurons) were CB_1/OX_1-ir, and all counted OX_1R-ir neurons were also CB_1R-ir (Fig. 2E).

2.2. Central OX_1R mediates i.c. orexin-A evoked cardiovascular response

As shown in Fig. 3A and B, orexin-A (0.1, 1, 3 nmol, i.c.) elicited dose-related pressor and tachycardic responses in conscious rats (*n*=4) in comparison to vehicle treated group, which agrees with reported studies (Chen et al., 2000; Samson et al., 1999). We then identified a dose of the selective OX_1R antagonist (SB-408124) that adequately blocked the central OX_1R-mediated pressor response. In this experiment, 3 groups of conscious freely moving rats (*n*=5–8) received i.c. injection of one of the following treatment pairs (vehicle+3 nmol orexin-A), (10 nmol SB-408124+vehicle) or (10 nmol SB-408124+3 nmol orexin-A). The SB-408124 dose and the 10 min interval between the successive injections were based on a preliminary study. Baseline MAP and HR were similar and were not significantly influenced by pretreatment with SB-408124 compared to vehicle (Table 1). As shown in Fig. 3C and D, the pressor and tachycardic responses elicited by the highest orexin-A dose (3 nmol, i.c.) were abrogated by prior blockade of central OX_1R with SB-408124 (10 nmol; i.c.).

2.3. Central OX_1R blockade attenuates WIN55,212-2 evoked pressor response

In this experiment, we investigated the effect of prior central OX_1R blockade (SB-408124; 10 nmol, i.c.), 10 min earlier, on the pressor response elicited by WIN55,212-2 (15 μg, i.c.) (*n*=8) and the effect of prior central CB_1R blockade (AM251; 30 μg, i.c.), 30 min earlier, on the pressor response elicited by orexin-A (3nmol, i.c.) (*n*=7). The AM251 dose and time interval were based on our previous findings (Ibrahim and Abdel-Rahman, 2011, 2012b). Further, we directly investigated the role of RVLM OX_1R in the pressor response caused by the activation of RVLM CB_1R. In this latter experiment, two groups of conscious rats (*n* = 6) received WIN55,212-2 (0.1 μg/200 pmol) 10 min after vehicle (control) or SB-408124 (1 nmol; based on preliminary experiment); injections were made unilaterally into the right RVLM in 80 nl and vehicle microinjection in such volume had no impact on BP in our previous studies. The intra-RVLM WIN55,212-2 dose was based on our previous studies (Ibrahim and Abdel-Rahman, 2012b). As shown in Figs. 4A and 5A, central OX_1R blockade, with intracisternal (10 nmol) or direct intra-RVLM (1 nmol) SB-408124, virtually abolished ($P<0.05$) the CB_1R-mediated pressor response caused by i.c. (15 μg) or direct intra-RVLM (0.1 μg) WIN55,212-2 microinjection. On the other hand, selective central CB_1R blockade (AM251; 30 μg, i.c.) had no significant effect on the orexin-A (3 nmol, i.

c.)-evoked pressor response (Fig. 4C). The heart rate responses followed the same trend (Figs. 4 and 5).

2.4. Central CB_1R activation (WIN55,212-2) increases RVLM orexin-A

The objective of this experiment was to test the hypothesis that elevation in orexin-A level in the RVLM mediates the pressor response elicited by central CB_1R activation. A total of 17 rats, divided into 4 groups (n=3–5 each), were used for the measurement of RVLM orexin-A level in treatment and control groups according to the protocol followed in the first part of Section 2.3 above and in our previous studies (Ibrahim and Abdel-Rahman, 2012a, 2012b). Two groups received WIN55,212-2 (15 μg, i.c.) 30 min after the CB_1R antagonist AM251 (30 μg; i.c.) or vehicle. The other two groups received the vehicle 30 min after AM251 (30 μg, i.c.) or vehicle. The rats were euthanized 10–15 min after WIN55,212-2 or vehicle injection, and the brains were collected. This time interval coincided with the peak of WIN55,212-2-evoked pressor response as shown in Fig. 4 and in our previous studies (Ibrahim and Abdel-Rahman, 2012a, 2012b). To gain direct evidence that the activation of RVLM CB_1R increases local orexin-A level, we measured orexin-A in microinjected and contralateral (control) RVLM tissues collected at the end of the second part of Section 2.3 above. Intracisternal WIN55,212-2 significantly (P<0.05) increased RVLM orexin-A level and AM251 abrogated this response (Fig. 4E); these neurochemical responses paralleled the BP responses (Fig. 4A). Similarly, intra-RVLM WIN55,212-2 (0.1 μg) significantly (P<0.05) increased BP (Fig. 5A) and RVLM orexin-A level (Fig. 5B) but prior RVLM OX_1R blockade (SB-408124) only abrogated the pressor response (Fig. 5A and B). There were no significant differences between orexin-A levels in the contralateral (non-injected, control) RVLM (Fig. 5B) and the RVLM of intracisternal vehicle-treated rats (Fig. 4E).

2.5. Central OX_1R blockade abrogated CB_1R enhancement of RVLM ERK1/2 and nNOS phosphorylation

In this study we tested the hypothesis that OX_1R signaling is implicated in the enhancement of RVLM ERK1/2 and nNOS phosphorylation; the latter is an important neurochemical event in the central CB_1R (WIN55,212-2)-evoked pressor response (Ibrahim and Abdel-Rahman, 2012a, 2012b). RVLM tissues collected at the conclusion of cardiovascular measurements in Section 2.3 were used for the measurement of the levels of phosphorylated ERK1/2 and nNOS (normalized to their respective total protein) in rats treated with WIN55,212-2 in the absence or presence (n=5 each) of SB-408124 or vehicle (n=4). Central CB_1R activation (WIN55,212-2) significantly (P<0.5) enhanced the phosphorylation of RVLM nNOS (Fig. 6A) and ERK1/2 (Fig. 6B), and prior OX_1R blockade (SB-408124) abrogated (P<0.05) these neurochemical responses (Fig. 6).

3. Discussion

The most important findings of the current study are (i) CB_1R and OX_1R are colocalized, along with orexin-A fibers, in tyrosine hydroxylase expressing (C1) neurons in the RVLM, (ii) central CB_1R activation by i.c. or intra-RVLM WIN55,212-2 increased BP and RVLM orexin-A level, (iii) central CB_1R blockade (AM251) abrogated WIN55,212-2 evoked increases in RVLM orexin-A level but had no effect on the central OX_1R (orexin-A)-

mediated pressor response, (iv) central OX_1R blockade (SB-408124) abrogated the increases in RVLM ERK1/2 and nNOS phosphorylation and BP, but not the increase in RVLM orexin-A level, caused by central CB_1R activation. Our recent findings implicated enhanced phosphorylation of RVLM ERK1/2 and nNOS in central CB_1R-mediated pressor response (Ibrahim and Abdel-Rahman, 2012a, 2012b). Further, reported findings implicated RVLM OX_1R signaling in central orexin-A-evoked pressor response (Chen et al., 2000; Ciriello et al., 2003a; Huang et al., 2010; Machado et al., 2002; Shahid et al., 2012) possibly via nNOS/NO signaling (Xiao et al., 2013). We tested the hypothesis that brainstem OX_1R signaling underlies the central CB_1R-mediated phosphorylation of RVLM nNOS and ERK1/2 and the subsequent pressor response.

We have recently established that i.c. WIN55,212-2 increases BP in conscious rats, at least partly, via CB_1R-mediated neurochemical mechanisms in the RVLM (Ibrahim and Abdel-Rahman, 2011, 2012a, 2012b). Similarly, reported studies implicated the RVLM in the pressor response elicited by i.c. (Chen et al., 2000; Zhang et al., 2005) or intra-RVLM orexin injection (Chen et al., 2000; Ciriello et al., 2003a; Huang et al., 2010; Shahid et al., 2012). However, these orexin studies were conducted in anesthetized rats and disagreed on which peptide (orexin-A or B) and receptor (OX_1R or OX_2R) played the major role in the response. Therefore, it was imperative that we generate new data necessary for testing our hypothesis. First, while the colocalization of CB_1R/OX_1R is evident in the feeding control area of the hypothalamus (Matias et al., 2008), we report the first evidence for similar colocalization in the RVLM (Fig. 2). Importantly, a potential functional link between the two receptors was their colocalization, along with orexin-A fibers, in the C1 area of the RVLM (Figs. 1 and 2). These findings support the reported projections of the excitatory orexinergic neurons to different brain areas including the medullary cardiovascular regulatory nuclei, the RVLM and the nucleus tractus solitarius (Machado et al., 2002; Puskás et al., 2010; Shahid et al., 2012; Zheng et al., 2005). Reported studies have shown differential orexinergic projections to various brain areas including dorsal raphe nucleus, ventral tegmental area, the vestibular complex and cerebellum, nucleus tractus solitaries, nucleus ambiguus, dorsal medulla (Ciriello et al., 2003b; Ciriello and Caverson, 2014; Del Cid-Pellitero and Garzon, 2014; Harrison et al., 1999; Lee et al., 2005). However, the authors are not aware of studies that demonstrated differential sub-hypothalamic origin of orexin projections specific to the RVLM. It is possible that orexin neurons projecting to RVLM originate from the cardiovascular pressor perifornical and medial lateral hypothalamus (Harrison et al., 1999; Zheng et al., 2005); yet this possibility requires further investigation. Interestingly, a recent study, which used anterograde tracing with viral vectors, demonstrated the projection of the RVLM C1 cell group to the entire orexin-rich region of the hypothalamus (Bochorishvili et al., 2014). Second, our integrative studies demonstrated the ability of i.c. orexin-A to elicit dose-related pressor response in our conscious rat model system (Fig. 3). We concluded that orexin-A produces the pressor response via OX_1R because the response was abrogated by prior central OX_1R blockade with SB-408124 (Fig. 3). The latter conclusion is supported by similar SB-334867 attenuation of intra-RVLM orexin-A evoked pressor response (Shahid et al., 2012). We then utilized the selected SB-408124 dose to directly test our hypothesis that brainstem OX_1R signaling plays a pivotal role in the CB_1R-mediated pressor response.

The WIN55,212-2 evoked pressor response in the present study ultimately results from sympathoexcitation caused by indirect modulation of converging excitatory and inhibitory inputs, which control the sympathetic neuronal activity in the RVLM (Ibrahim and Abdel-Rahman, 2011, 2012b; Padley et al., 2003; Pilowsky and Goodchild, 2002). Our novel hypothesis that release of the sympathoexcitatory peptide orexin-A within the RVLM underlies the central CB_1R-mediated pressor response is based on reported interaction between the CB_1R and orexin systems in vitro (Ellis et al., 2006; Hilairet et al., 2003; Ward et al., 2011a, 2011b) and in in vivo feeding studies (Crespo et al., 2008; Verty et al., 2009). Perhaps a potential functional interaction between these two systems in a neuronal pool that controls sympathetic outflow (RVLM) has remained unexplored because the limited in vivo studies on the two systems have focused on orexin A-containing neurons in the lateral hypothalamic area (De Lecea et al., 1998; Sakurai et al., 1998).

We present the first evidence that prior blockade of central OX_1R (SB-408124) attenuated the central CB_1R (WIN55,212-2)-evoked pressor and bradycardic responses (Fig. 4A and B). This finding, which is in line with the molecular and behavioral (feeding) studies (Crespo et al., 2008; Ellis et al., 2006; Hilairet et al., 2003; Ward et al., 2011a, 2011b), suggests the dependence of the central CB_1R–mediated pressor response on central OX_1R signaling. Realizing that other brain areas, that send projections to the brainstem, might have been involved in these observed effects following i.c. injections of administered drugs (Fig. 4), we directly injected the drugs into the RVLM in a subsequent experiment. The abolition of the intra-RVLM WIN55,212-2-evoked pressor response by prior intra-RVLM SB-408124 (Fig. 5) directly supports the involvement of RVLM OX_1R signaling in the pressor response caused by RVLM CB_1R activation. Additionally, we adopted two biochemical and molecular approaches to further substantiate the involvement of OX_1R signaling in CB_1R-mediated responses. First, we present the first evidence that i.c. WIN55,212-2 significantly elevated RVLM orexin-A level (Figs. 4E and 5B), which coincides with the CB_1R–evoked increase in plasma norepinephrine levels in our previous study (Ibrahim and Abdel-Rahman, 2011). Second, the enhanced phosphorylation of RVLM ERK1/2 and nNOS, which is implicated in the i.c. WIN55,2122-2 (CB_1R)-mediated pressor response (Ibrahim and Abdel-Rahman, 2012a, 2012b), was abrogated by prior OX_1R blockade (SB-408124) (Fig. 6). It is imperative to note that: (i) nNOS/NO is implicated in orexin-A evoked sympathoexcitatory effect in the RVLM (Xiao et al., 2013), and (ii) ERK1/2 dependent phosphorylation of nNOS in the RVLM is implicated in sympathoexcitation (Martins-Pinge et al., 1999, 2007; Mayorov, 2007; Nassar and Abdel-Rahman, 2008). Collectively, the pharmacological and biochemical findings strongly suggest role for RVLM OX_1R signaling in the neurochemical mechanism that underlies the central (RVLM) CB_1R-mediated pressor response.

The crosstalk between CB_1R and OX_1R reported in vitro (Ellis et al., 2006; Hilairet et al., 2003; Ward et al., 2011a, 2011b) may be pertinent to the in vivo interaction between the two systems. For example, orexin-A mediated feeding was abrogated by CB_1R blockade (Crespo et al., 2008) and administration of CB_1R antagonist AM251 caused reduction in food intake and orexin-A immunoreactivity in LH (Merroun et al., 2015). Furthermore, in rats conditioned place preference (CPP) studies via stimulating lateral hypothalamus (LH), concurrent administration of CB_1R antagonist (AM251) in nucleus accumbens altered the SB334867 (OX_1R selective antagonist)-mediated attenuation of LH stimulation-induced

CPP (Fatahi et al., 2015). Our findings are partly consistent with this reported reciprocal inter-dependence of the CB_1R and OX_1R signaling in vitro and in functional/feeding in vivo studies (Crespo et al., 2008; Ellis et al., 2006; Hilairet et al., 2003; Jäntti et al., 2014; Ward et al., 2011a, 2011b). While blockade of central OX_1R (SB-408124) abrogated the central CB_1R-mediated responses (Fig. 4A), blockade of central CB_1R (AM251) had no effect on orexin-A evoked BP response (Fig. 4C). This latter observation suggests that central OX_1R (orexin-A)-mediated pressor response is not dependent on CB_1R signaling in our model system, and raises the possibility that the reported "reciprocal" CB_1R-OX_1R interaction might be organ/tissue specific. However, the exact mechanism of this interaction within the RVLM remains to be elucidated because it might involve heterodimer formation (Ellis et al., 2006; Jäntti et al., 2014) in addition to elevating orexin-A levels (this study).

As briefly discussed above, the measurement of orexin-A in the RVLM (Figs. 4E and 5B), constituted an important step for direct testing of our hypothesis. We demonstrated, for the first time, that central CB_1R activation significantly elevated RVLM orexin-A level, which coincided with the peak of the pressor response, and the rise in plasma norepinephrine levels (Ibrahim and Abdel-Rahman, 2011). The latter notion links increased sympathetic activity to CB_1R-mediated increase in RVLM orexin-A level, a finding that is supported by a sympathoexcitatory role for orexin-A in the RVLM (Huang et al., 2010; Shahid et al., 2012; van den Top et al., 2003). However, it was important to verify that the WIN55,212-2 evoked increase in RVLM-orexin-A level was CB_1R-mediated and plays a causal role in the pressor response. This objective was achieved by demonstrating that selective blockade of central CB_1R (AM251) abrogated the WIN55,2122-2 evoked elevations in RVLM orexin-A (Fig. 4E), and in BP in our previous study (Ibrahim and Abdel-Rahman, 2011). Equally important, we showed that localized RVLM blockade of OX_1R attenuated WIN55,212-2-evoked pressor response (Fig. 5A) but not the associated elevation in RVLM orexin-A (Fig. 5B). Notably, while the rapid rise in RVLM-orexin-A level precludes a possible effect of CB_1R activation on the peptide synthesis, such rise likely results from local alterations in peptide turnover, degradation and/or hydrolysis of its precursor preproorexin (Gallmann et al., 2006); more studies are needed to investigate this possibility in the RVLM. Nonetheless, these findings suggest that elevation in the RVLM orexin-A is CB_1R-mediated and contributes to the central CB_1R-mediated pressor response.

In conclusion, we provide the first neurochemical and pharmacological evidence for a functional dependence of central CB_1R-mediated pressor response on RVLM orexin system. CB_1R activation caused elevation in RVLM orexin-A level at the peak of the pressor response and the latter was abrogated by prior blockade of central OX_1R. On the other hand, the orexin-A (OX_1R)-evoked pressor response was not affected by prior central CB_1R blockade. In support of these pharmacological findings, colocalization studies unraveled co-localization of orexin-A/OX_1R with CB_1R in TH-ir neurons in the RVLM. Along with our recent findings (Ibrahim and Abdel-Rahman, 2012a, 2012b), the present molecular and BP findings suggest that elevation of orexin-A level within the RVLM constitutes a primary event in a neurochemical cascade that leads to CB_1R-evoked nNOS/ERK1/2 phosphorylation, and ultimately increased BP (Fig. 7). The findings support the involvement RVLM CB_1R-OX_1R in blood pressure regulation and perhaps in pathological conditions such as hypertension. The identification of new strategies that target both CB_1/OX_1

receptors (Zhang et al., 2010a, 2010b) will advance our understanding of the pathophysiological role of their interaction as well as in developing new therapeutics for the treatment of hypertension.

4. Experimental procedures

4.1. Animals

Male Sprague-Dawley rats (300–350 g, Charles River, Raleigh, NC) were housed two per cage in a room with controlled environment at a constant temperature of 23±1°C, humidity of 50±10% and a 12:12-h light/dark cycle. Food (Prolab Rodent Chow, Granville Milling, Creedmoor, NC) and water were provided ad libitum. All surgical, experimental, and animal care procedures were performed in accordance with, and approved by, the Institutional Animal Care and Use Committee and in accordance with the *Guide for the Care and Use of Laboratory Animals* (Institute of Laboratory and Animal Resources, 2010).

4.2. Intra-arterial, intracisternal and intra-RVLM cannulation

Surgeries were performed under sterile conditions and ketamine (9 mg/100 g) and xylazine (1 mg/100 g, i.p.) anesthesia as detailed in our previous study (Ibrahim and Abdel-Rahman, 2011, 2012b) where an arterial catheter for blood pressure (BP) measurement was placed into the abdominal aorta via the femoral artery and a guide cannula for intracisternal or intra-RVLM injections. Each rat received i.m. buprenorphine (30 μg/ kg; Rickitt and Colman, Richmond, VA) and s.c. penicillin G benzathine and penicillin G procaine in an aqueous suspension (100,000 U/kg; Durapen; Vedco, Inc., Overland Park, KS) and was housed in a separate cage for at least five days to fully recover.

4.3. Blood pressure and heart rate measurements

On the day of the experiment, the arterial catheter was flushed with heparinized saline (100 IU/ml), connected to a Gould-Statham pressure transducer (Oxnard-CA) and the procedures detailed in our previous studies (Ibrahim and Abdel-Rahman, 2011) were utilized for BP and heart rate (HR) measurements in conscious unrestrained rats recorded by ML870 (PowerLab 8/30), and analyzed using LabChart (v.6) pro software (ADInstruments, Colorado Spring, CO). BP and HR were allowed to stabilize at baseline before drug/vehicle administration and were continuously monitored until euthanasia. Identification of the RVLM was based on obtaining a pressor response elicited by injecting 1 nmol L-glutamate at the beginning of each experiment and histological verification for both intra-RVLM and i.c. at the end of the experiment following microinjection of fast green dye. Animals that did not meet the verification procedures were excluded from data interpretation as detailed in our previous studies (Ibrahim and Abdel-Rahman, 2012b). Brain tissues were collected to conduct biochemical studies as detailed below.

4.4. Immunofluorescence

Naïve untreated rats (n=4) were deeply anaesthetized as described above, transcardially perfused with 4% paraformaldehyde in phosphate buffered saline (PBS), the brain was isolated and left in the same buffer overnight at 4 °C. Brains were then . transferred to 30% sucrose in PBS and kept in 4 °C till they sank. Coronal brainstem (30 μm) sections, rostrally

from −12.6 to −11.8 mm relative to bregma (Chen et al., 2010), were processed for multiple label immunofluorescence colocalization studies as previously described (Ibrahim and Abdel-Rahman, 2011, 2012b). The brainstem sections were incubated in blocking buffer (PBS buffer containing 0.2% Tween 20 (PBST) and 5% normal donkey serum) at 4 °C for 2 h, then with mixtures of mouse anti-tyrosine hydroxylase (TH) (1:500; Millipore, Temecula, CA), goat anti-CB_1R (1:200; Santa Cruz Biotech, Santa Cruz, CA) with either rabbit anti-OX_1R (1:100; Millipore, Temecula, CA) or rabbit anti-orexin-A (1:500; EMD Chemicals, San Diego, CA) for 48 h. After washing 3 times in PBST, sections were then incubated with a mixture of fluorophores-conjugated secondary antibodies containing FITC donkey anti-mouse, Cy3 donkey anti-rabbit and Cy5 donkey anti-goat (1:200; Jackson ImmunoResearch, West Grove, PA) to simultaneously visualize TH, CB_1R and OX-A or OX_1R, respectively. Finally, sections were mounted on glass slides, cover slipped with Vectashield (Vector Laboratories, Burlingame, CA) and sealed with nail polish. Incubating tissues with cocktails of the primary antibodies and their corresponding antigenic peptides resulted in abolished immunoreactivity and confirmed antibody specificities to their target proteins that were also reported in previous studies (Giuliano et al., 2009; Kalifa et al., 2011; Shahid et al., 2012).

Brainstem coronal sections (15–24/animal; *n*=4) were analyzed to determine the co-localization of TH/OX_1R/CB_1R–ir through the caudal-rostral ventrolateral medulla (−12.6 to −11.8 from bregma) using a Zeiss LSM 510 confocal microscope (Thornwood, New York). The RVLM (Fig. 1A) was defined as the area ventral to the NA, medial to the spinal trigeminal tract and lateral to the pyramidal tract or the inferior olive (Chen et al., 2010). Cell counting was confined to those optical sections that contained CB_1/OX_1 receptors labeling and TH staining (Fig. 1B). First, with the 543 nm for Cy3 and 633 nm for Cy5; respectively, used to detect CB_1R and OX_1R immunofluorescent labeling turned off, each 0.5 μm optical section was examined for cells stained with TH via turning on the excitation channel 488 nm, which were then numbered. Cells were considered TH-ir if the entire cell body was visible in a 1 μm thick optical section. After identifying TH-ir neurons, the channels used to detect CB_1R and OX_1R immunolabeling were turned on individually and each identified cell throughout the optical stack was analyzed for CB_1/OX_1 receptors immunoreactivity. A neuron was considered triple labeled for TH/CB_1R/OX_1R if labeling of CB_1R varicosities (circular punctate profiles) and/or OX_1R existed within the boundaries of the TH-ir neuron according to reported criteria (Wilson-Poe et al., 2012). Neurons that were immunoreactive only for CB_1 and/or OX_1 receptors were counted separately. Zeiss LSM Image Browser software was used to assign color profiles to fluorescence and adjusting images used for publication for optimal brightness and contrast.

4.5. Western blot analysis

Phosphorylated and total nNOS and ERK1/2 were measured as reported in our recent studies (Ibrahim and Abdel-Rahman, 2012a, 2012b). Brain tissues were collected 30 min after administration of WIN55,212-2 or its vehicle, at the conclusion of BP measurement following euthanasia with lethal dose of pentobarbital sodium (>100 mg/kg) followed by decapitation. RVLM Tissue was collected bilaterally using a 0.75-mm punch tool , (Stoelting Co., Wood Dale, IL), approximately −12.6 to −11.8 mm relative to bregma (Chen et al., 2010).

4.6. Measurement of orexin-A

RVLM orexin-A level was quantified with a standard ELISA kit (EK-003–30; Phoenix Pharmaceutical, Burlingame, CA) in accordance with the manufacturer's procedures and as reported (Feng et al., 2007, 2012; Olszanecka-Glinianowicz et al., 2007). Briefly, four groups of animals treated as described under experimental design were euthanized 10–15 min after WIN55,212-2 or vehicle injection; brains were removed, flash frozen in 2-methylbutane (cooled on dry ice for at least 30 min), and stored at −80 °C until use. RVLM Tissue was, unless otherwise specified, collected bilaterally using a 0.75-mm punch tool (Stoelting Co., Wood Dale, IL), approximately −12.6 to −11.8 mm relative to bregma (Chen et al., 2010). Samples were then acid-extracted, and protein was quantified using a standard Bio-Rad protein assay system (Bio-Rad Laboratories, Hercules, CA) and assayed in duplicates for orexin-A. Values, for each sample, were averaged and expressed as ng/mg total protein. The minimum detection concentration for this assay is typically 0.22 ng/ml, with a linear range of 0.22–2.28 ng/ml. The mean intra-assay coefficient of variance was <4.0% and the mean inter-assay coefficient of variance was <12.0%.

4.7. Drugs and reagents

WIN55,212-2, SB-408124 and DMSO were purchased from Sigma-Aldrich (St. Louis, MO). AM251 was purchased from Cayman Chemical (Ann Arbor, MI). The emulsifier Alkamuls EL620 (polyethoxylated castor oil) was purchased from Rhodia (Cranbury, NJ). WIN55,212-2 and AM251 were dissolved in (1:1:18) mixture of DMSO/Alkamuls/sterile saline. Orexin-A peptide was purchased from Phoenix Pharmaceutical (Burlingame, CA) and dissolved in sterile saline. SB-408124 dissolved in 10% DMSO in sterile saline. As none of these vehicles significantly changed the basal levels of MAP and HR, we refer to all of them as vehicle as in our previous studies (Ibrahim and Abdel-Rahman, 2012a, 2012b). Drug or vehicle injections were made into the cisterna magnum or, intra-RVLM when specified, in conscious unrestrained rats as detailed in our previous studies (Ibrahim and Abdel-Rahman, 2011, 2012a, 2012b).

4.8. Statistical analysis

Mean arterial pressure (MAP) and HR are expressed as mean ± S.E.M. change from their respective baseline values after the pretreatment and prior to WIN55,212-2, orexin-A or their respective vehicles injections. Data were then analyzed by repeated measures ANOVA using SPSS 16.0 statistical package for Windows as detailed in our previous studies (Ibrahim and Abdel-Rahman, 2012a). The values in the table represent baseline MAP or HR before administering the vehicle, while the after values in the table represent the MAP and HR prior to WIN or orexin. Responses in the graphs following WIN or orexin are relative to the "after" values included in the table. Western blot data for each protein were expressed as percent of control (vehicle alone) value, and analyzed by unpaired t-test using GraphPad Prism V5 for Windows®. Further, one-way ANOVA, followed by multiple comparison post-hoc, was conducted in the studies on WIN55,212-2 in the presence or absence of AM251 or SB-408124 on RVLM orexin-A level. $P<0.05$ was considered significant.

Acknowledgments

The authors acknowledge the technical assistance provided by Ms. Kui Sun.

This work was supported by the National Institutes of Health National Institute on Alcohol Abuse and Alcoholism [Grant 2R01 AA07839-19] and in part by the El-Minia Faculty of Pharmacy via a scholarship provided by the Egyptian Government (Scholarship Missions Program, Ministry of Higher Education) to Badr M. Ibrahim.

Abbreviations

AM251	N-(piperidin-1-yl)-5-(4-iodophenyl)-1-(2,4-dichlorophenyl)-4-methyl-1 H-pyrazole-3-carboxamide
BP	blood pressure
CB_1R	cannabinoid receptor 1
ERK1/2	extracellular signal-regulated kinase1/2
p-ERK1/2	phosphorylated ERK1/2
HR	heart rate
MAP	mean arterial pressure
nNOS	neuronal nitric oxide synthase
OX_1R	Orexin receptor 1
RVLM	rostral ventrolateral medulla
SB-408124	[N-(6,8-Difluoro-2-methyl-4-quinolinyl)-N'-[4-(dimethylamino) phenyl] urea
WIN55,212-2	(R)-(+)-[2,3-dihydro-5-methyl-3[(4-morpholinyl)methyl]pyrrolo[1,2,3-de]-1,4-benzoxazinyl]-(1-naphthalenyl) methanone mesylate salt

REFERENCES

Bochorishvili G, Nguyen T, Coates MB, Viar KE, Stornetta RL, Guyenet PG. The orexinergic neurons receive synaptic input from C1 cells in rats. J. Comp. Neurol. 2014; 522:3834–3846. [PubMed: 24984694]

Chalmers J, Pilowsky P. Brainstem and bulbospinal neurotransmitter systems in the control of blood pressure. J. Hypertens. 1991; 9:675–694. [PubMed: 1680911]

Chen C-Y, Bonham AC, Dean C, Hopp FA, Hillard CJ, Seagard JL. Retrograde release of endocannabinoids inhibits presynaptic GABA release to second-order baroreceptive neurons in NTS. Autonom. Neurosci. 2010; 158:44–50.

Chen CT, Hwang LL, Chang JK, Dun NJ. Pressor effects of orexins injected intracisternally and to rostral ventrolateral medulla of anesthetized rats. Am. J. Physiol. - Regul. Integr. Comp. Physiol. 2000; 278:R692–R697. [PubMed: 10712290]

Ciriello J, Li Z, de Oliveira CV. Cardioacceleratory responses to hypocretin-1 injections into rostral ventromedial medulla. Brain Res. 2003a; 991:84–95. [PubMed: 14575880]

Ciriello J, McMurray JC, Babic T, de Oliveira CVR. Collateral axonal projections from hypothalamic hypocretin neurons to cardiovascular sites in nucleus ambiguus and nucleus tractus solitarius. Brain Res. 2003b; 991:133–141. [PubMed: 14575885]

Ciriello J, Caverson MM. Hypothalamic Orexin-A (Hypocretin-1) Neuronal Projections to the Vestibular Complex and Cerebellum in the Rat. 2014; 1579:20–34.

Crespo I, Heras RGD, Fonseca FRD, Navarro M. Pretreatment with subeffective doses of Rimonabant attenuates orexigenic actions of orexin A-hypocretin 1. Neuropharmacology. 2008; 54:219–225. [PubMed: 17889909]

De Lecea L, Kilduff TS, Peyron C, Gao X-B, Foye PE, Danielson PE, Fukuhara C, Battenberg ELF, Gautvik VT, Bartlett FS, Frankel WN, van den Pol AN, Bloom FE, Gautvik KM, Sutcliffe JG. The hypocretins: hypothalamus-specific peptides with neuroexcitatory activity. Proc. Natl. Acad. Sci. USA. 1998; 95:322–327. [PubMed: 9419374]

Del Cid-Pellitero E, Garzon M. Hypocretin1/orexinA-immunoreactive axons form few synaptic contacts on rat ventral tegmental area neurons that project to the medial prefrontal cortex. BMC Neurosci. 2014; 15:105. [PubMed: 25194917]

Drew GM, Mitchell VA, Vaughan CW. Glutamate spillover modulates GABAergic synaptic transmission in the rat midbrain periaqueductal grey via metabotropic glutamate receptors and endocannabinoid signaling. J. Neurosci. 2008; 28:808–815. [PubMed: 18216189]

Ellis J, Pediani JD, Canals M, Milasta S, Milligan G. Orexin-1 receptor-cannabinoid CB1 receptor heterodimerization results in both ligand-dependent and -independent coordinated alterations of receptor localization and function. J. Biol. Chem. 2006; 281:38812–38824. [PubMed: 17015451]

Fatahi Z, Assar N, Mahmoudi D, Pahlevani P, Moradi M, Haghparast A. Functional Interaction Between the Orexin-1 and CB1 Receptors Within the Nucleus Accumbens in the Conditioned Place Preference Induced by the Lateral Hypothalamus Stimulation. 2015; 132:42–48.

Feng P, Vurbic D, Wu Z, Strohl KP. Brain orexins and wake regulation in rats exposed to maternal deprivation. Brain Res. 2007; 1154:163–172. [PubMed: 17466285]

Feng XM, Mi WL, Xia F, Mao-Ying QL, Jiang JW, Xiao S, Wang ZF, Wang YQ, Wu GC. Involvement of spinal orexin A in the electroacupuncture analgesia in a rat model of post-laparotomy pain. BMC Complement. Altern. Med. 2012; 12:225. [PubMed: 23173601]

Freund TF, Katona I, Piomelli D. Role of endogenous cannabinoids in synaptic signaling. Physiol. Rev. 2003; 83:1017–1066. [PubMed: 12843414]

Gallmann E, Arsenijevic D, Williams G, Langhans W, Spengler M. Effect of intraperitoneal CCK-8 on food intake and brain orexin-A after 48 h of fasting in the rat. Regul. Peptides. 2006; 133:139–146.

Giuliano M, Pellerito O, Portanova P, Calvaruso G, Santulli A, De Blasio A, Vento R, Tesoriere G. Apoptosis induced in HepG2 cells by the synthetic cannabinoid WIN: involvement of the transcription factor PPARgamma. Biochimie. 2009; 91:457–465. [PubMed: 19059457]

Greenhough A, Patsos HA, Williams AC, Paraskeva C. The cannabinoid Δ9-tetrahydrocannabinol inhibits RAS-MAPK and PI3K–AKT survival signalling and induces BAD-mediated apoptosis in colorectal cancer cells. Int. J. Cancer. 2007; 121:2172–2180. [PubMed: 17583570]

Harrison TA, Chen CT, Dun NJ, Chang JK. Hypothalamic orexin A-immunoreactive neurons project to the rat dorsal medulla. Neurosci. Lett. 1999; 273:17–20. [PubMed: 10505641]

Herkenham M, Lynn AB, Johnson MR, Melvin LS, de Costa BR, Rice KC. Characterization and localization of cannabinoid receptors in rat brain: a quantitative in vitro autoradiographic study. J. Neurosci. 1991; 11:563–583. [PubMed: 1992016]

Hilairet S, Bouaboula M, Carriere D, Le Fur G, Casellas P. Hypersensitization of the Orexin 1 receptor by the CB1 receptor: evidence for cross-talk blocked by the specific CB1 antagonist, SR141716. J. Biol. Chem. 2003; 278:23731–23737. [PubMed: 12690115]

Huang H, Acuna-Goycolea C, Li Y, Cheng HM, Obrietan K, van den Pol AN. Cannabinoids excite hypothalamic melanin-concentrating hormone but inhibit hypocretin/ orexin neurons: implications for cannabinoid actions on food intake and cognitive arousal. J. Neurosci. 2007; 27:4870–4881. [PubMed: 17475795]

Huang S-C, Dai YW, Lee YH, Chiou LC, Hwang LL. Orexins depolarize rostral ventrolateral medulla neurons and increase arterial pressure and heart rate in rats mainly via orexin 2 receptors. J. Pharmacol. Exp. Ther. 2010; 334:522–529. [PubMed: 20494957]

Ibrahim BM, Abdel-Rahman AA. Role of brainstem GABAergic signaling in central cannabinoid receptor evoked sympathoexcitation and pressor responses in conscious rats. Brain Res. 2011; 1414:1–9. [PubMed: 21840505]

Ibrahim BM, Abdel-Rahman AA. Differential modulation of brainstem PI3K/Akt and ERK1/2 signaling underlies WIN55,212-2 centrally-mediated pressor response in conscious rats. J. Pharmacol. Exp. Ther. 2012a; 340:11–18. [PubMed: 21946192]

Ibrahim BM, Abdel-Rahman AA. Enhancement of rostral ventrolateral medulla neuronal nitric-oxide synthase-nitric-oxide signaling mediates the central cannabinoid receptor 1-evoked pressor response in conscious rats. J. Pharmacol. Exp. Ther. 2012b; 341:579–586. [PubMed: 22366659]

Jäntti MH, Mandrika I, Kukkonen JP. Human orexin/ hypocretin receptors form constitutive homo- and heteromeric complexes with each other and with human CB1 cannabinoid receptors. Biochem. Biophys. Res. Commun. 2014; 445:486–490. [PubMed: 24530395]

Kalifa S, Polston EK, Allard JS, Manaye KF. Distribution patterns of cannabinoid CB1 receptors in the hippocampus of APPswe/PS1DeltaE9 double transgenic mice. Brain Res. 2011; 1376:94–100. [PubMed: 21192920]

Lee HS, Park SH, Song WC, Waterhouse BD. Retrograde study of hypocretin-1 (orexin-A) projections to subdivisions of the dorsal raphe nucleus in the rat. Brain Res. 2005; 1059:35–45. [PubMed: 16153616]

Machado BH, Bonagamba LG, Dun SL, Kwok EH, Dun NJ. Pressor response to microinjection of orexin/hypocretin into rostral ventrolateral medulla of awake rats. Regul. Peptides. 2002; 104:75–81.

Martins-Pinge MC, Araujo GC, Lopes OU. Nitric oxide-dependent guanylyl cyclase participates in the glutamatergic neurotransmission within the rostral ventrolateral medulla of awake rats. Hypertension. 1999; 34:748–751. [PubMed: 10523354]

Martins-Pinge MC, Garcia MR, Zoccal DB, Crestani CC, Pinge-Filho P. Differential influence of iNOS and nNOS inhibitors on rostral ventrolateral medullary mediated cardiovascular control in conscious rats. Autonom. Neurosci. -Basic Clin. 2007; 131:65–69.

Matias I, Cristino L, Di Marzo V. Endocannabinoids: some like it fat (and sweet too). J. Neuroendocrinol. 2008; 20(Suppl. 1):S100–S109.

Mayorov DN. Nitric oxide synthase inhibition in rostral ventrolateral medulla attenuates pressor response to psychological stress in rabbits. Neurosci. Lett. 2007; 424:89–93. [PubMed: 17709184]

Merroun I, El Mlili N, Martinez R, Porres JM, Llopis J, Ahabrach H, Aranda P, Sanchez Gonzalez C, Errami M, Lopez-Jurado M. Interaction between orexin A and cannabinoid system in the lateral hypothalamus of rats and effects of subchronic intraperitoneal administration of cannabinoid receptor inverse agonist on food intake and the nutritive utilization of protein. J. Physiol. Pharmacol. 2015; 66:181–190. [PubMed: 25903949]

Nassar N, Abdel-Rahman AA. Brainstem phosphorylated extracellular signal-regulated kinase 1/2-nitric-oxide synthase signaling mediates the adenosine A2A–dependent hypotensive action of clonidine in conscious aortic barodenervated rats. J. Pharmacol. Exp. Ther. 2008; 324:79–85. [PubMed: 17934014]

Olszanecka-Glinianowicz M, Zahorska-Markiewicz B, Kocelak P, Janowska J, Semik-Grabarczyk E. Plasma orexin and ghrelin response to the oral glucose tolerance test in obese women. Endokrynol. Pol. 2007; 58:422–425. [PubMed: 18058738]

Padley JR, Li Q, Pilowsky PM, Goodchild AK. Cannabinoid receptor activation in the rostral ventrolateral medulla oblongata evokes cardiorespiratory effects in anaesthetised rats. Br. J. Pharmacol. 2003; 140:384–394. [PubMed: 12970095]

Pilowsky PM, Goodchild AK. Baroreceptor reflex pathways and neurotransmitters: 10 years on. J. Hypertens. 2002; 20:1675–1688. [PubMed: 12195099]

Piomelli D. The molecular logic of endocannabinoid signalling. Nat. Rev. Neurosci. 2003; 4:873–884. [PubMed: 14595399]

Puskás N, Papp RS, Gallatz K, Palkovits M. Interactions between orexin-immunoreactive fibers and adrenaline or noradrenaline-expressing neurons of the lower brainstem in rats and mice. Peptides. 2010; 31:1589–1597. [PubMed: 20434498]

Sakurai T, Amemiya A, Ishii M, Matsuzaki I, Chemelli RM, Tanaka H, Williams SC, Richardson JA, Kozlowski GP, Wilson S, Arch JRS, Buckingham RE, Haynes AC, Carr SA, Annan RS, McNulty DE, Liu W-S, Terrett JA, Elshourbagy NA, Bergsma DJ, Yanagisawa M. Orexins and orexin

receptors: a family of hypothalamic neuropeptides and G protein-coupled receptors that regulate feeding behavior. Cell. 1998; 92:573–585. [PubMed: 9491897]

Samson WK, Gosnell B, Chang JK, Resch ZT, Murphy TC. Cardiovascular regulatory actions of the hypocretins in brain. Brain Res. 1999; 831:248–253. [PubMed: 10412003]

Shahid IZ, Rahman AA, Pilowsky PM. Orexin A in rat rostral ventrolateral medulla is pressor, sympatho-excitatory, increases barosensitivity and attenuates the somato-sympathetic reflex. Br. J. Pharmacol. 2012; 165:2292–2303. [PubMed: 21951179]

Shirasaka T, Nakazato M, Matsukura S, Takasaki M, Kannan H. Sympathetic and cardiovascular actions of orexins in conscious rats. Am. J. Physiol. 1999; 277:R1780–R1785. [PubMed: 10600926]

van den Top M, Nolan MF, Lee K, Richardson PJ, Buijs RM, Davies CH, Spanswick D. Orexins induce increased excitability and synchronisation of rat sympathetic preganglionic neurones. J. Physiol. 2003; 549:809–821. [PubMed: 12702746]

Verty ANA, Boon WM, Mallet PE, McGregor IS, Oldfield BJ. Involvement of hypothalamic peptides in the anorectic action of the CB1 receptor antagonist rimonabant (SR 141716). Eur. J. Neurosci. 2009; 29:2207–2216. [PubMed: 19490094]

Ward RJ, Pediani JD, Milligan G. Ligand-induced internalization of the orexin OX1 and cannabinoid CB1 receptors assessed via N-terminal SNAP and CLIP-tagging. Br. J. Pharmacol. 2011a; 162:1439–1452. [PubMed: 21175569]

Ward RJ, Pediani JD, Milligan G. Heteromultimerization of cannabinoid CB1 receptor and orexin OX1 receptor generates a unique complex in which both protomers are regulated by orexin A. J. Biol. Chem. 2011b; 286:37414–37428. [PubMed: 21908614]

Wilson-Poe AR, Morgan MM, Aicher SA, Hegarty DM. Distribution of CB1 cannabinoid receptors and their relationship with mu-opioid receptors in the rat periaqueductal gray. Neuroscience. 2012; 213:191–200. [PubMed: 22521830]

Xiao F, Jiang M, Du D, Xia C, Wang J, Cao Y, Shen L, Zhu D. Orexin A regulates cardiovascular responses in stress-induced hypertensive rats. Neuropharmacology. 2013; 67:16–24. [PubMed: 23147417]

Zhang W, Fukuda Y, Kuwaki T. Respiratory and cardiovascular actions of orexin-A in mice. Neurosci. Lett. 2005; 385:131–136. [PubMed: 15941620]

Zhang Y, Gilliam A, Maitra R, Damaj MI, Tajuba JM, Seltzman HH, Thomas BF. Synthesis and biological evaluation of bivalent ligands for the cannabinoid 1 receptor. J. Med. Chem. 2010a; 53:7048–7060. [PubMed: 20845959]

Zhang, Y.; Perrey, D.; Gilmour, BP.; Langston, T.; Warner, K.; Thomas, BF. Synthesis and evaluation of bivalent ligands for CB1-OX1 receptor heterodimers; Research Triangle Park, NC, USA. Proceedings of the 20th Annual Symposium on the Cannabinoids. International Cannabinoid Research Society; 2010b. p. 47

Zheng H, Patterson LM, Berthoud HR. Orexin-A projections to the caudal medulla and orexin-induced c-Fos expression, food intake, and autonomic function. J. Comp. Neurol. 2005; 485:127–142. [PubMed: 15776447]

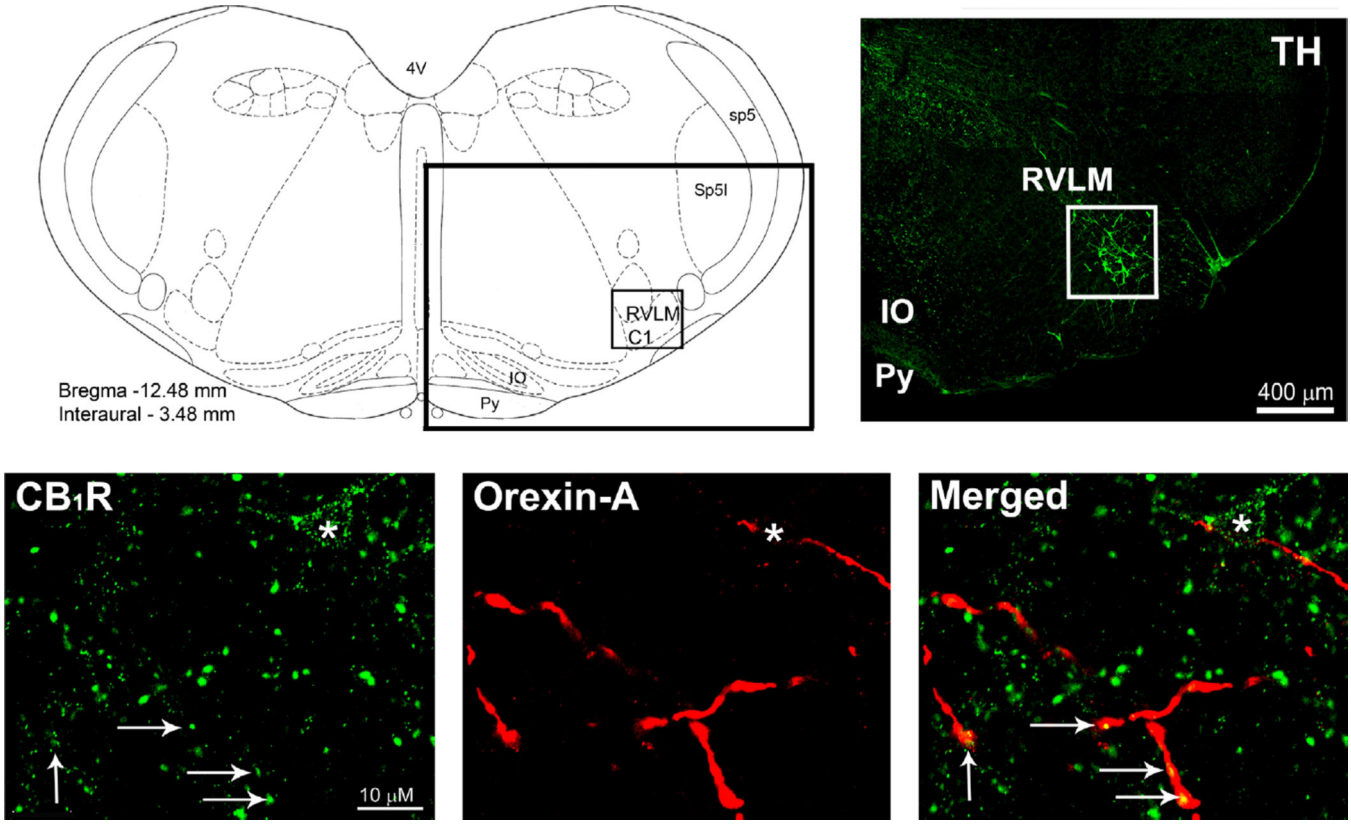

Fig. 1.

(A) Schematic presentation of coronal brainstem section showing the rostral ventrolateral medulla site (RVLM; black box) and the adjacent anatomical landmarks −12.48 mm from the bregma. (B) Photomicrograph representing the black box in (A) depicting tyrosine hydroxylase (TH)-ir neurons (Greenhough et al., 2007) in the RVLM (white box). (C) Confocal images depicting labeling of CB_1R (green) and orexin-A varicose like nerve fibers (red). A merged image shows apposition (asterisks) or colocalization (arrows) of CB_1R immunoreactive varicosities and orexin-A immunoreactive fibers. 4V: fourth ventricle; IO: Inferior Olive; Py: Pyramidal tract; Sp5: spinal trigeminal nucleus, Sp5I: Sp5 interpolar part.

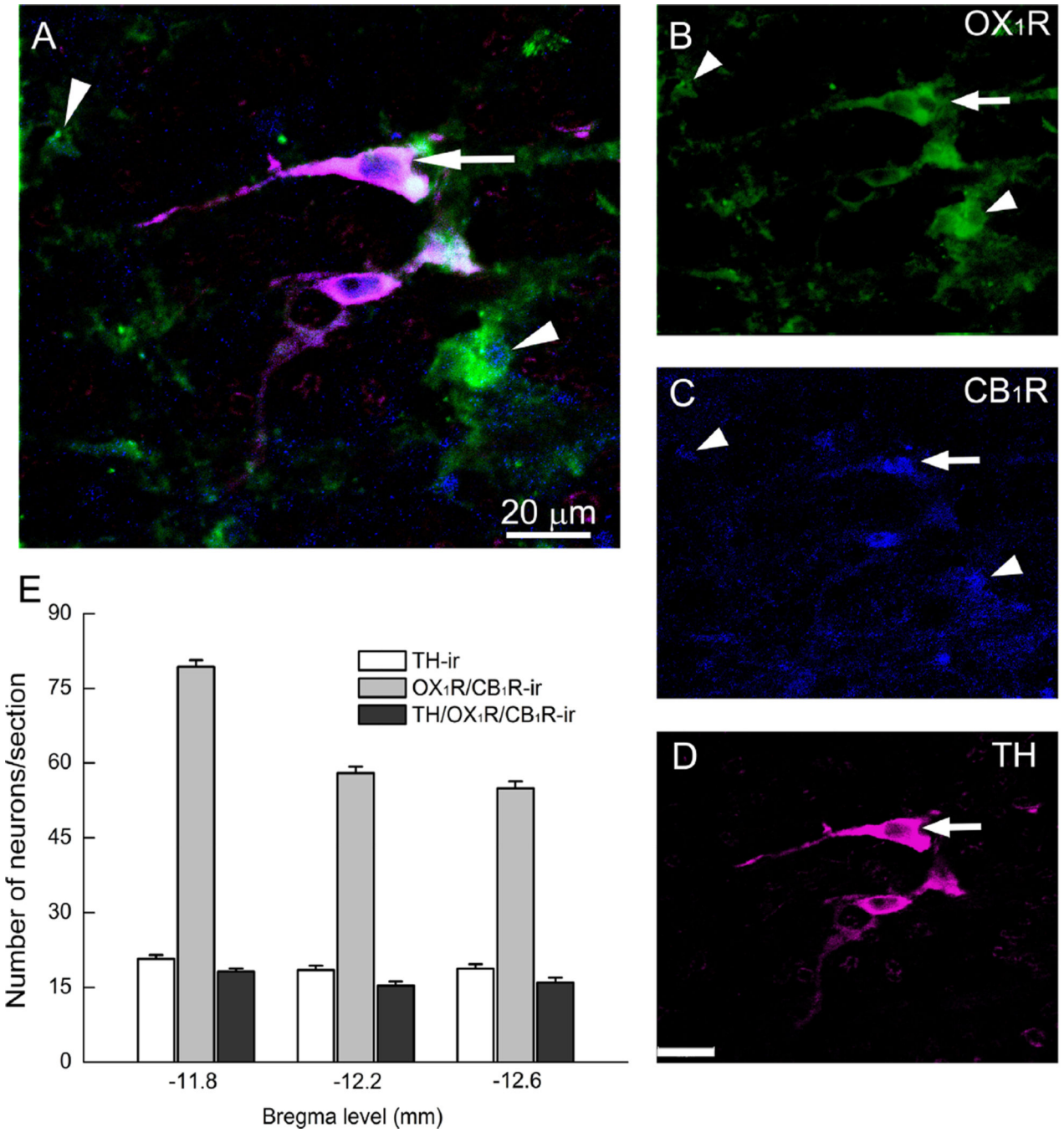

Fig. 2.

Confocal images depicting co-localization (A) of OX_1R (B), CB_1R (C) and tyrosine hydroxylase (TH)-ir neurons (D) in the rostral ventrolateral medulla (RVLM). The arrows indicate colocalization of CB_1R/OX_1R in cell bodies of TH-ir neurons; the arrowheads neuronal structures immunoreactive to CB_1/OX_1 receptors that lack TH staining. (E) Quantitative presentation of rostrocaudal distribution of TH-ir neurons, OX_1R/CB_1R-ir, and $TH/OX_1R/CB_1R$-ir profiles in brainstem coronal sections. The bar graphs represent averages

of neurons counted in 15–24 sections/animal (n=4) within the VLM area –11.8 mm rostral to – 12.6 mm caudal from the bregma.

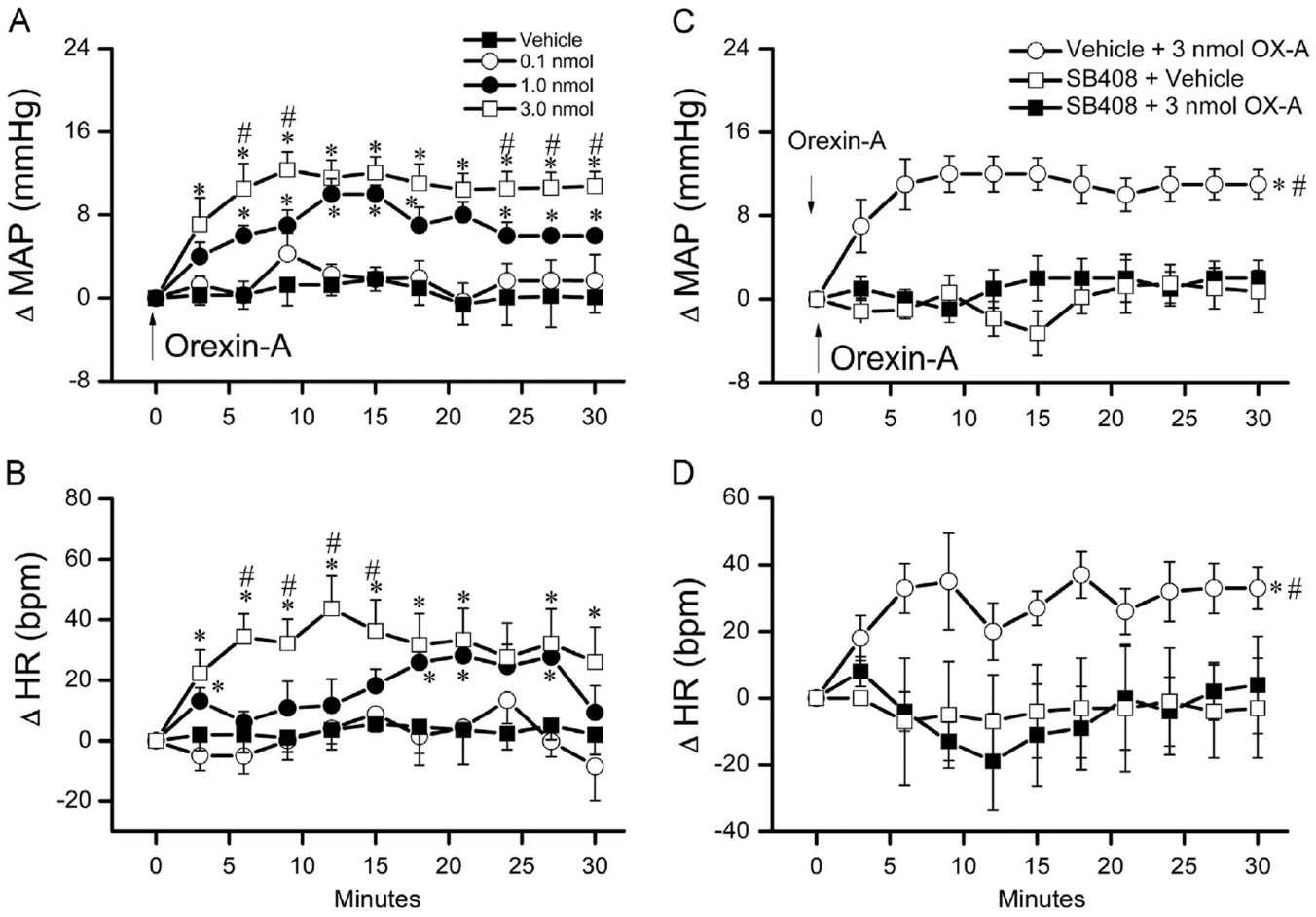

Fig. 3.

Dose-related changes in mean arterial pressure (MAP) (A) and heart rate (HR) (B) evoked by intracisternal orexin-A (0.1, 1 or 3 nmol) or vehicle in conscious unrestrained rats (n=4). Values are mean±S.E.M. * and #p<0.05 versus respective vehicle or “0.1 nmol orexin-A” values. Time course of changes in MAP (C), and HR (D) evoked by i.c. 3 nmol of orexin-A (vehicle+orexin-A) or its vehicle, indicated by the arrow (top panel), in conscious rats pretreated, 10 min earlier, with the selective OX_1R antagonist SB-408124 (10 nmol, i.c.) (SB-408124+orexin-A) or vehicle (SB-408124+Veh). Values are mean±S.E. M. of 5–8 observations. * and #p<0.05 versus respective “SB-408124+Veh” and “SB-408124+orexin-A” values.

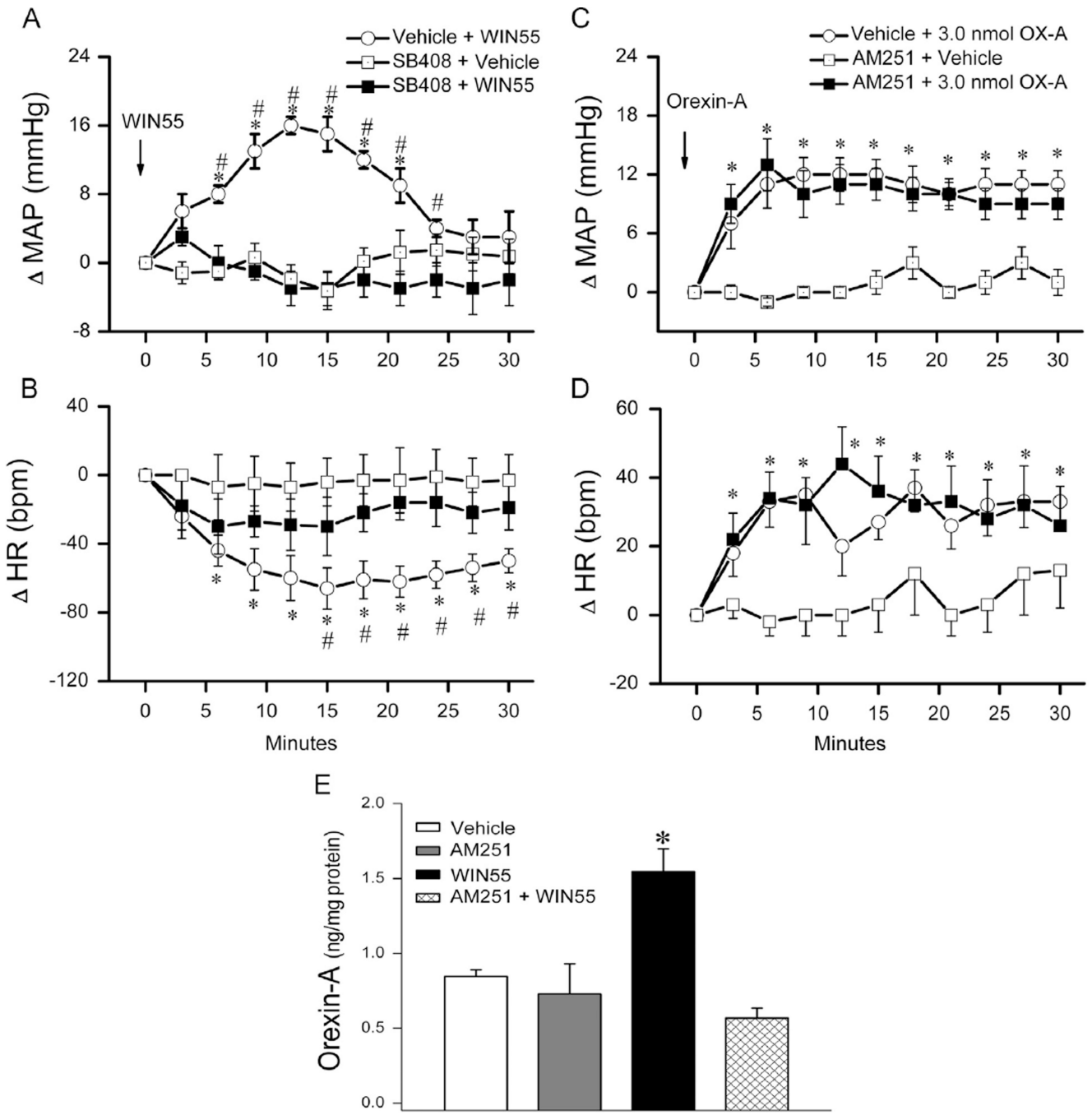

Fig. 4.

Time course of changes in mean arterial pressure (MAP) (A), heart rate (HR) (B) evoked by intracisternal (i.c.) WIN55,212-2 (15 μg) (Veh+WIN55) or its vehicle, indicated by the arrow (top panel), in conscious rats pretreated, 10 min earlier, with the selective OX_1R antagonist SB-408124 (10 nmol, i.c.) (SB-408124+WIN55) or vehicle (SB-408124+Veh). Values are mean±S.E.M. of 5 to 8 observations. * and #$p<0.05$ versus respective "SB-408124+Veh" and "SB-408124+WIN55" values. Time course of changes in MAP (C), HR (D) evoked by orexin-A (3 nmol, i.c.) (Veh+orexin-A), (reblotted from Fig. 3) or its

vehicle, indicated by the arrow (top panel), in conscious rats pretreated 30 min earlier with selective CB_1R antagonist AM251 (30 μg, i.c.) (AM251+orexin-A) or equal volume of vehicle (AM251+vehicle). Values are mean±S.E.M. of 5–8 observations. *P<0.05 versus respective (AM251+vehicle) values. (E) Changes in RVLM orexin-A level, determined by ELISA as detailed under methods, in four additional groups of animals that received one of the following i.c. treatments: (vehicle; n=3), (vehicle+WIN55,212-2; n=5), (AM251+vehicle; n=4) or (AM251+WIN55,212-2; n=5). Animals were sacrificed at 10 min, a time that coincided with the peak of the WIN55,212-2-evoked pressor response. Bar graphs represent mean±S.E.M. Data analyzed by one-way ANOVA followed by Bonferroni comparison test. *P<0.05 compared to “vehicle” and “AM251+WIN55,212-2” values.

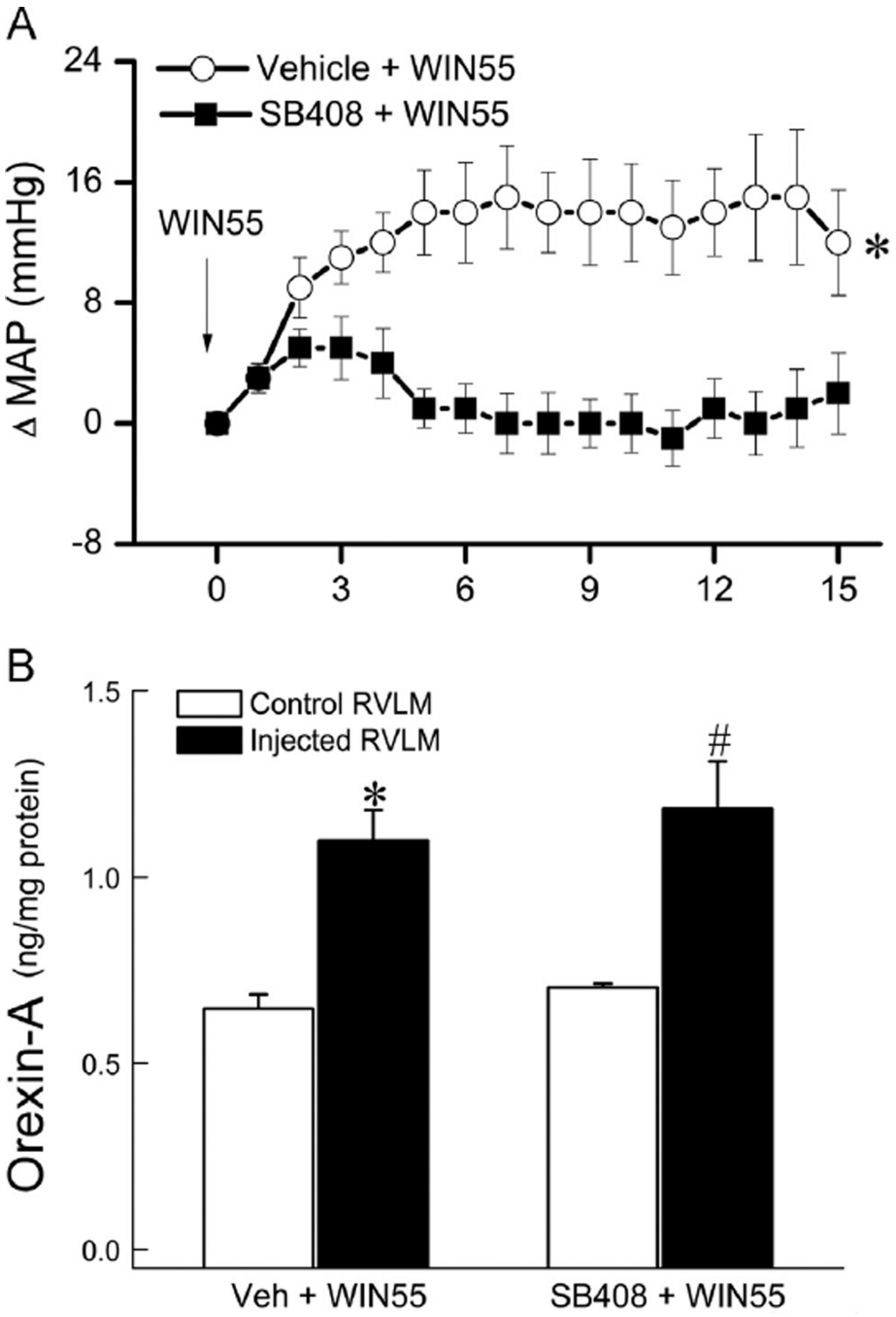

Fig. 5.

Time course of changes in mean arterial pressure (MAP) (A) evoked by intra-RVLM WIN55,212-2 (0.1 μg/ 200 pmol) (Veh+WIN55) in conscious rats pretreated, 10 min earlier, with the selective OX_1R antagonist SB-408124 (1 nmol, intra-RVLM) (SB-408+WIN55). Values are mean±S. E.M. of 6 observations. *p< 0.05 versus respective "SB-408124+WIN55" values. (B) Changes in orexin-A level in treated (microinjected side; black bars) or non-treated (contralateral control side; open bars) RVLM of two groups of animals that received one of the following intra-RVLM treatments: (vehicle+WIN55,212-2;

n=6) or (SB-408124+WIN55,212-2; *n*=6). Bar graphs represent mean±S. E.M. Data analyzed by unpaired Student-t test. * or #*P*<0.05 compared to the control RVLM.

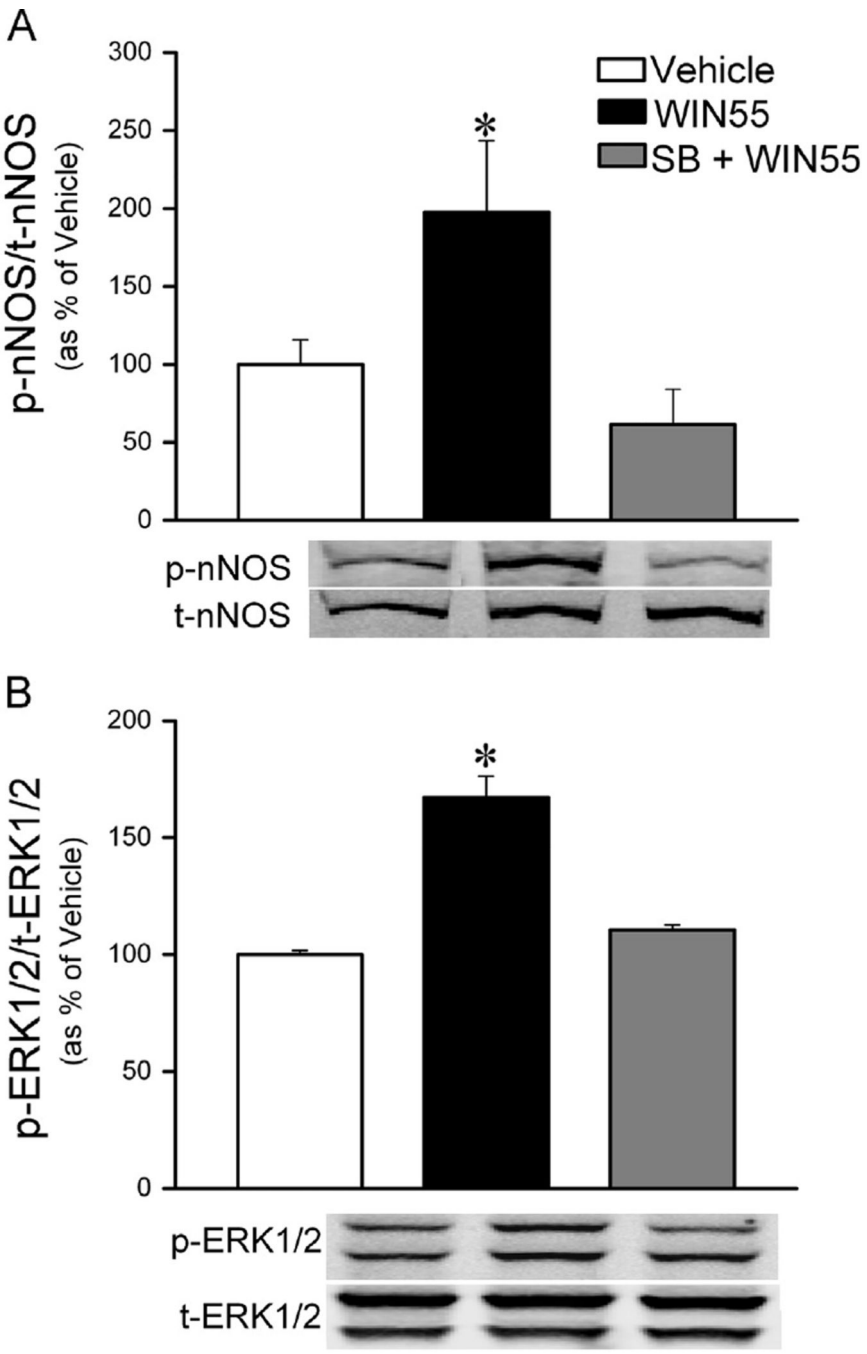

Fig. 6.

Changes in rat RVLM nNOS (A) and ERK1/2 (B) phosphorylation following intracisternal (i.c.) WIN55,212-2 (15 μg) or its vehicle in animals pretreated with sterile saline or the OX_1R antagonist SB-408124 (10 nmol, i.c.). Data are presented as integrated density ratio of phosphorylated (p-nNOS) or (p-ERK1/2) to the corresponding total (t-nNOS) or (t-ERK1/2) protein, and expressed as percent of control (vehicle) value. Values are mean±S.E.M. of 4–5 observations. *p<0.05 versus vehicle values, respectively.

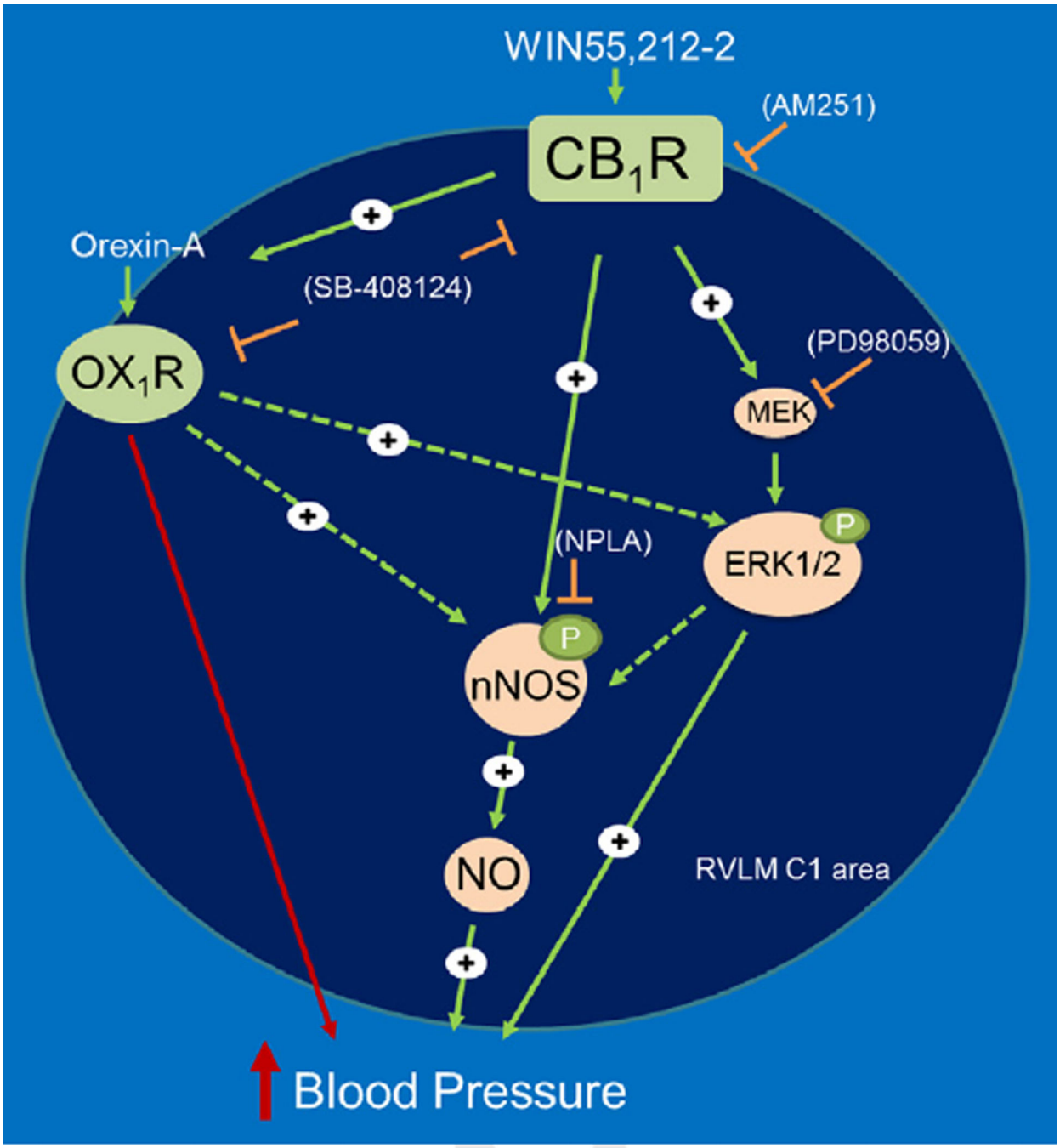

Fig. 7.

Schematic presentation of the functional dependence of central CB_1R-mediated pressor response on brainstem OX_1R/orexin-A signaling. Central CB_1R (WIN55,212-2) or OX_1R (orexin-A) activation increases blood pressure in conscious freely moving rats (Figs. 3–5), and central CB_1R activation increased RVLM orexin-A level (Figs. 4 and 5) and enhances ERK1/2 and nNOS phosphorylation in the RVLM (Fig. 6). The proposed model system is further supported by our previous neurochemical and pharmacological findings following intracisternal or intra-RVLM microinjection of the CB_1R agonist WIN55,212-2 (Ibrahim

and Abdel-Rahman, 2011, 2012a, 2012b), which implicated ERK1/2 and nNOS phosphorylation and enhanced NO generation in the RVLM in WIN55,212-2 evoked pressor response. Solid arrows indicate findings based on our current and previous studies, while dashed arrows indicate proposed signaling based on reported in vitro findings, but not tested in this model (see text for details).

Table 1

Lack of effect of CB1R (AM251) or Orexin receptor (SB-408124) antagonist on mean arterial pressure (MAP) and heart rate (HR) in conscious rats. "*Before*" represents baseline MAP and HR values while "*After*" represents MAP and HR values after intracisternal (i.c.) AM251, SB-408124 or vehicle *prior* to i.c. WIN55,212-2, orexin-A or vehicle. Values are means±S.E.M.

Treatment	*n*	MAP (mmHg)		HR (bpm)	
		Before	After	Before	After
Vehicle	3	115.0±6.0	110.0±6.0	395±12	386±11
Vehicle+15 μg WIN55,212-2	5	111.3±3.0	108.0±5.0	375±10	350±11
AM251+vehicle	4	108±6.0	114.3±3.0	360±11	390±10
AM251+15 μg WIN55,212-2	5	112.0±6.0	117.0±6.0	356±15	376±15
Vehicle+orexin-A	6	111.3±3.0	112.0±3.0	375±10	363±13
SB-408124+vehicle	5	113.0±4.0	110.0±4.0	398±16	390±20
SB-408124+orexin-A	8	117.0±6.0	115.0±4.0	400±12	410±12
SB-408124+WIN55,212-2	8	110.0±4.0	111.0±2.0	392±16	388±16
AM251+orexin-A	7	109.0±3.0	113±3.0	360±18	375±18